STUDY ON THE EFFECT OF WIDTH AND SLOPE OF LARGE CROSS-SECTION TUNNEL ON CRITICAL VELOCITY OF FIRE

Su Liu*[1]

[1]School of Resources and Civil Engineering, Northeastern University ,Shengyang 110819
[*]Corresponding author; E-mail: suliuvip@163.com

Abstract: *when a tunnel fire occurs, due to the difference of tunnel width and slope, both smoke countercurrent length distribution law and critical velocity will become different, and these two are very important parameters in tunnel longitudinal ventilation design. Therefore, for the design of smoke control and longitudinal ventilation of the tunnel, based on actual highway tunnel size, this paper established and ran a series of numerical simulations through FDS simulation software to study tunnel width and slope's effect on smoke countercurrent length and critical velocity. The results of this paper show that smoke countercurrent length decreases with tunnel slope's increase and increases with tunnel width's increase. Through dimensionless analysis, the prediction formulas of smoke countercurrent length and critical wind speed of large cross-section tunnel about tunnel width, slope and height are modified and established. The research conclusions can provide a theoretical basis for the longitudinal ventilation design, smoke prevention and exhaust measures and personnel evacuation in large cross-section tunnel fires.*

Key words*: large cross-section tunnel; fire; tunnel width; tunnel slope; critical velocity*

1. Introduction

In recent years, with our country's speedy development and world economy's soaring, modern science and technology are constantly improving, and the construction projects of tunnels and underground spaces are constantly developing. A large number of long tunnels with a cross-sectional area of more than 50 m^2 have been built at home and abroad. At the same time, due to different geological environments, in order to reduce the construction cost and construction difficulty, tunnels often have a certain inclination angle [1-3]. For example, Fangdoushan tunnel has a length of 7790 m on the right hole and 7590 m on the left hole. The tunnel's cross-sectional area is between 42 m^2-72 m^2 and the slope is in the range of 22°-24°. Zhenxishan tunnel is 2635 m long, 9.6 m wide, 5.8 m high and slope is 25°. Erlangshan tunnel is 4176 m long, 9.5 m wide and 5.7 m high, with a slope of 6 °. The baseline tunnel in St. Gotha, Switzerland, is 16286 m long, 9.3 m wide, 7.5 m high and has a slope of 5.5 °.

While tunnel brings convenience to traffic, it often has great fire safety hazards. Because of its own special structural characteristics, while a fire takes place, smoke quickly spreads around, it is extremely difficult to discharge, resulting in the rapid consumption of fresh air in the tunnel, the accumulation of heaps of noxious and poisonous gases, reduced visibility, extremely difficult evacuation and rescue [4-5]. For example, in 2005, a natural vehicle accident occurred in the Freis

tunnel in France, resulting in 22 deaths and serious damage to the tunnel. In 2015, a rear-end fire occurred in the Futuyu tunnel, killing 12 people and damaging 8 trucks and 1 bus. In May 2017, a vehicle fire occurred in Taojiazhuang tunnel, killing 13 people. Besides, 2 people were injured when 2 cars collided in a fire in Netherlands' Benelux tunnel in 2019. A vehicle fire broke out in Guanyinshan Tunnel on March 1, 2022, injuring 1 person and damaging 5 vehicles. The specific tunnel fire accident in Taojiazhuang tunnel is shown in Fig. 1, from which we can see that when a tunnel fire occurs, it often produces heaps of smoke. Besides, above tunnel fires cause a large number of people to fail to escape, mainly because fire smoke is not discharged in time, so tunnel fire smoke's control is of great significance. The main ways to control tunnel fire smoke discharge are natural ventilation, transverse ventilation, longitudinal ventilation and mixed ventilation. Because longitudinal ventilation has the advantages of high ventilation efficiency and low cost of construction and maintenance, longitudinal ventilation is adopted in most tunnels [6-7], such as Hongtiguan tunnel, Nibashan tunnel and Caihongling tunnel.

Fig. 1 Tunnel fire accident (pictures from Xinhuanet)

When a tunnel fire occurs, smoke countercurrent is a special smoke movement phenomenon, longitudinal ventilation's critical velocity is the minimum ventilation speed to prevent smoke countercurrent to fire source's upstream. Smoke countercurrent length refers to the distance of fire smoke flowing upstream along the fire source when ventilation speed is less than critical velocity. Critical velocity refers to longitudinal ventilation speed when smoke countercurrent length is zero [8]. When tunnel's longitudinal ventilation speed is greater than or equal to critical velocity, the fire smoke flows downstream, which can ensure smoothness and safety of upstream position of fire source and prevent smoke from harming people and vehicles upstream. Meanwhile, it provides fire rescue and personnel evacuation a safe passage [9]. Therefore, the research on critical velocity and fire smoke countercurrent length is an significant basis for tunnel fire ventilation design and smoke control.

As one of tunnel fire's most significant phenomena, smoke countercurrent length has been widely studied by heaps of scholars. Weng et al. [10] analyzed slope's effect on smoke countercurrent length, pointed out that smoke countercurrent length decreases with tunnel slope's increase. Weng et al. [11] and Zhao et al. [12] analyzed fires in tunnels with different widths, obtained prediction formulas of smoke countercurrent length and critical velocity in tunnels with different width-height ratios. Ingason et al. [13] and Wu et al. [14] executed experimental studies on reduced-size fire in tunnels with different slopes, obtained and established a critical velocity that can just prevent upwind backflow of smoke. Chow et al. [15] conducted reduced-size fire experiments on a series of tunnels with different slopes to study slope's effect on smoke countercurrent length. Ji et al. [16-17] studied the tunnel with different inclined angles under natural ventilation, carried out the reduced-size fire experiment, acquired the relation between upwind smoke countercurrent length and slope. Fan et al. [18] indicated that increasing inclined tunnel's angle would be beneficial to promote chimney effect and reduce fire

smoke's backflow through the research and analysis of smoke caused by inclined tunnel. Through the analysis of inclined tunnel fire, Shafee and Yozgatligil [19] indicated that tunnel angle has definite effect on tunnel smoke diffusion. Zhang et al. [20] studied the relationship between smoke countercurrent length and slope by establishing 9 tunnel models with slopes of 0, 1%, 2%, 3%, 4%, 5%, 6%, 7% and 8%. The results showed that with tunnel slope's increase, smoke countercurrent length decreased, and a prediction model considering tunnel slope and height was proposed.

Thomas [21] first proposed critical velocity in 1968 and obtained the empirical formula of critical velocity. Then Oka and Atkinson [22] established a segmented dimensionless critical velocity formula through heaps of reduced-size propane fire experiments. Wu and Bakar [14] and Li et al [23] carried out a sequence of reduced-size fire experiments on tunnels with distinct widths. Their research shows that tunnel fire's critical velocity varies with tunnel width. Ko et al. [24] studied tunnel slope's effect on fire critical velocity through experiments, obtained the relation between critical velocity and tunnel tilt angle. Weng et al. [25] put forward the prediction formula of tunnel fire's critical velocity through 1:10 scale model experiment. Through experiments, Yi et al. [26] indicated there is a positive correlation between critical velocity and tunnel slope. Li and Ingason et al. [27-28] indicated that tunnel aspect ratio has definite effect on critical velocity. Li et al. [29] studied tunnel fires with 3%, 5% and 7% slopes through experiments in a 1:8 scaled tunnel model, and established corresponding numerical models. The critical velocity slope correction coefficient obtained has a linear correlation with tunnel slope. Jiang et al. [30] conducted reduced-size fire experiments on tunnels with a slope of -5%-5%. At the same time, they conducted numerical simulations through FDS simulation software. They concluded that tunnel slope's effect on critical velocity was not affected by fire source's heat release rate.

However, the above studies on tunnel fire critical velocity often do not consider whether tunnel section is a large section, and only consider tunnel slope or width's effect on critical velocity in a single variable. Therefore, it is valuable to study the coupling effect of the width and slope of large cross-section tunnel on critical velocity. In this paper, the coupling effect of width and slope of large cross-section tunnel on critical velocity is learnt by numeric simulation. The second section introduces the establishment of the numerical models. The third section analyzes the numerical experimental results of tunnel fires with different widths and slopes from the aspects of smoke countercurrent characteristics, smoke countercurrent length and critical velocity. The research outcomes can provide a theoretical basis for personnel rescue and fire ventilation of large-section tunnels with different widths and slopes.

2. Numerical simulation

Due to the limitations of experimental sites and conditions, many actual fire scene experiments are difficult to achieve. Therefore, a large number of researchers use a fire dynamics simulation software called FDS to study tunnel fires under different working conditions [31-34]. The FDS version used in this article is 6.7.

2.1. Fire scene design

The specific FDS fire models are shown in Fig. 2. In the numerical models, the tunnel lengths are 100 m, the tunnel heights are 5 m, the tunnel width d is 10 m, 12 m, 14 m, 16 m, 18 m and 20 m respectively, and tunnel slope γ is 0 °, 5 °, 10 °, 15 °and 20 ° respectively. In this paper, the downward gravity change is used to simulate the difference of tunnel inclination. In each simulation

model, the tunnel longitudinal ventilation speed is set to 1m/s and natural ventilation, the ventilation direction is blowing from the lower part of the tunnel to the higher part. Heaps of previous researches have demonstrated that [35], 0.1 m below tunnel ceiling is the maximal ceiling smoke temperature position. Therefore, in this paper, thermocouples are set at 0.1 m below the ceiling in each model's longitudinal center axis, and a group of velocity measuring points are set at 1.5 m of the characteristic height of human eyes. Both the distance between each group of thermocouples and the distance between velocity measuring points is 1 m. These measuring points measure the tunnel smoke temperature and velocity respectively, as displayed in Fig. 2 (a).

Cars are the most prevalent vehicles in road tunnels, and each car's heat release rate is approximately 3-5 MW. Therefore, 4 MW is selected as heat release rate for modeling. The fire source is situated in tunnel's center, with a distance of 50 m from both tunnel ports. It is stipulated that tunnel's left side is x=0 m. In the tunnel fire in this paper, under natural ventilation or longitudinal ventilation's action, air flows from tunnel's lower part to the higher part, so fire smoke below fire source is upwind and above the fire source is downwind, as displayed in Fig. 2 (b).

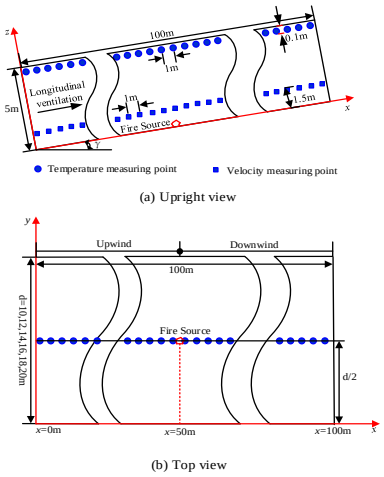

Fig. 2 Model and survey point layout

2.2. Initial and boundary conditions

In each numerical model, the initial ambient temperature is set to 20 ℃, the ambient pressure is set to an atmospheric pressure 101 kpa, and heptane is selected as the fire source fuel.

In numerical calculation process, the Dirichlet boundary is used as the open boundary condition at both tunnel ports, and boundary parameters are consistent with internal material properties. The homogeneous material "concrete" is used in the model tunnel, and its thermal properties are as follows: Density is 2280 kg/m^3. Specific heat is 1.04 kJ/ (kg·K). Electrical conductivity is 1.8 W/ (m·K). Emissivity is 0.9. Absorption coefficient is 50000 l/m. The ambient temperature is set to 20℃, the temperature of the tunnel side wall is consistent with the ambient temperature, and the tunnel boundary is set to natural ventilation conditions. According to the FDS instruction manual, the smooth Werner-Wengle (W-W) wall model is adopted in this paper.

2.3. Grid settings

According to previous studies, the division of mesh size of numerical model has an important influence on simulation results' accuracy. Pursuant to FDS user instruction manual written by

McGrattan et al. [36], it is suggested that the grid size range is 1/16~1/4 of characteristic diameter of the fire source D^*, where D^*can be calculated as follows:

$$D^* = （ Q/\rho_a c_p T_a \sqrt{g} ）^{2/5} \quad （1）$$

Where: D^* is fire source's characteristic diameter (m). Q is heat release rate (kW). ρ_a is ambient air density (kg/m^3). c_p is ambient air specific heat capacity at constant pressure (kJ/ (kg·K)). T_a is ambient air temperature (K). g is the gravitational acceleration (m/s^2).

According to the above formula (1), when heat release rate is 4 MW, characteristic diameter D^* is 1.62m, from which grid size can be selected from 0.10 m~0.41 m. Therefore, in this paper, four kinds of grid sizes in the range of 0.1 m to 0.4 m are selected for simulation and comparison. Fig. 3 demonstrates vertical temperature distribution at the upwind distance of 10 m from the fire source when tunnel inclination is 10 °and tunnel width is 10 m.

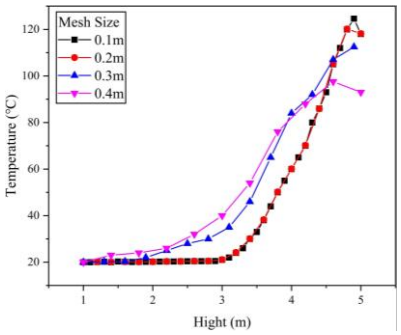

Fig. 3 Vertical distribution diagram of smoke temperature under different grid sizes

According to Fig. 3, when model grid size is 0.3 m and 0.4 m respectively, vertical temperature distribution curve of tunnel smoke varies greatly. When the model grid is 0.1 m and 0.2 m, tunnel smoke's vertical temperature distribution curve is very close, which shows that tunnel smoke's vertical temperature distribution curve is very close when the grid is less than 0.2 m. The accuracy of the simulation is not significantly improved, but the smaller the mesh size is, the longer the simulation time is. To save time and improve computer's running speed, when grid size is 0.2 m, the calculation results have high reliability and accuracy. At the same time, Long et al. [38] and Ji et al. [39] have done heaps of research on similar tunnel fire simulation, also used the grid size similar to this paper, as displayed in Table 1.

Table 1 Previous FDS numerical simulation research

References	Tunnel size/m	Heat release rate/MW	Grid size/m
Long et al.[38]	Length 200，width 10，height 5	20	0.2
Ji et al.[39]	Length 100，width10，height 5	3–15	0.167

According to the research, heptane can reach a stable state after a very short time of combustion. Therefore, in order to make smoke diffusion reach a stable state, simulation running time is set at 350 s. Fig. 4 shows the variation of flue gas temperature in the tunnel roof under the fire source with time at different longitudinal distances from the fire source. As can be seen from Figure 4, the longitudinal

ceiling temperature at different distances from the fire source reaches a stable state about 140s after the fire. In order to eliminate the influence of simulation time on simulation results, ensure the stability of all data. Therefore, we extract the steady-state average value of 200 s-350 s to study the large cross-section tunnel fire.

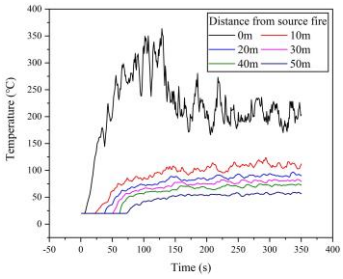

Fig. 4 Variation of flue gas temperature over time at different longitudinal distances from the downwind of the fire source

2.4. Verification of model results

In order to further verify the precision and reliability of the numerical model in this paper, a numerical model that is consistent with previous experimental conditions is established, and simulated values are compared with previous experimental results. Wu et al. [14] conducted a reduced-size tunnel fire experiment, tunnel size was 15 m long, 0.25 m high and 0.5 m wide. In this paper, a 1:20 tunnel numerical model is established by expanding the size scale. The mesh size is 0.2 m, the length is 100 m, the height is 5 m, and the width is 10 m. The ignition source uses heptane as fuel, and heat release rate is 4 MW.

Fig. 5 shows comparison between numerical simulation results and reduced-size tunnel fire experiment results of Wu et al. [14]. As can be seen from Fig. 5, numeric simulation consequences are very close to experimental results, indicating the dependability and accuracy of the model results established in this paper. Where V_c^* is dimensionless critical velocity and Q_c^* is dimensionless heat release rate of the fire source. The specific formula is as follows:

$$V_c^* = V/\sqrt{gH} \quad (2)$$

$$Q_c^* = Q/\rho_a c_p T_a \sqrt{g} H^{\frac{5}{2}} \quad (3)$$

In the above formula, V is tunnel ventilation velocity (m/s) and H is tunnel height (m).

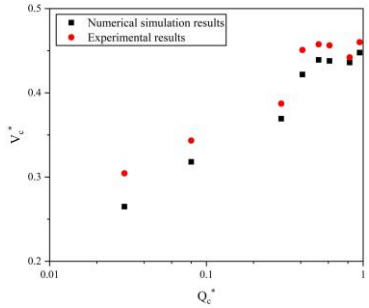

Fig. 5 Comparison between numerical simulation results and experimental results

3. Results and analysis

3.1. Effect of tunnel width and slope on smoke countercurrent length

The chimney effect is caused by temperature difference inside and outside the tunnel and tunnel height difference. The air velocity caused by chimney effect can promote or hinder the smoke flow to some degree.

Fig. 6 shows the airflow velocity v_{in} at tunnel entrance due to chimney effect under natural ventilation when tunnel has different width and slope. According to Fig. 6, air inflow velocity at entrance increases with tunnel slope's increase, and entrance's velocity changes significantly with tunnel width's narrowing. When tunnel width is 10-14 m, under the same slope condition, the velocity decreases significantly with tunnel width's increase. When tunnel width increases to 14-20 m, the velocity at the tunnel entrance also changes, but there is no obvious change as mentioned above.

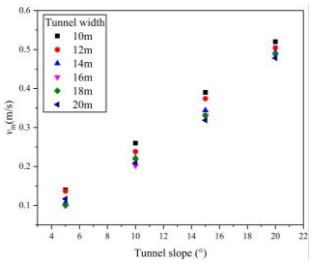

Fig. 6 Relation diagram between tunnel slope and inlet airflow velocity v_{in}

In order to further verify the relation between tunnel entrance's airflow velocity and the tunnel slope and width, Fig. 7 shows temperature distribution of tunnel cross section with different slopes and widths at the position where the distance from the tunnel lower port is x=1 m under the natural ventilation condition. It is visible from Fig. 7 (a) that when tunnel width is 14 m, with tunnel slope's increase, fire hot smoke layer's position gradually moves upward, the upper hot smoke layer gradually becomes thinner, and the lower cold air gradually thickens. According to Fig. 7 (b), when tunnel slope is 14 °, with tunnel width's increase, the hot smoke layer position gradually moves down, the upper hot smoke layer gradually thickens, and the lower cold air gradually thins. The main reason is that with tunnel slope's increase, tunnel chimney effect increases, air velocity at the entrance increases, and upwind flow of fire smoke is more and more hindered. With tunnel width's increase, tunnel entrance's air velocity decreases and fire smoke's diffusion increases.

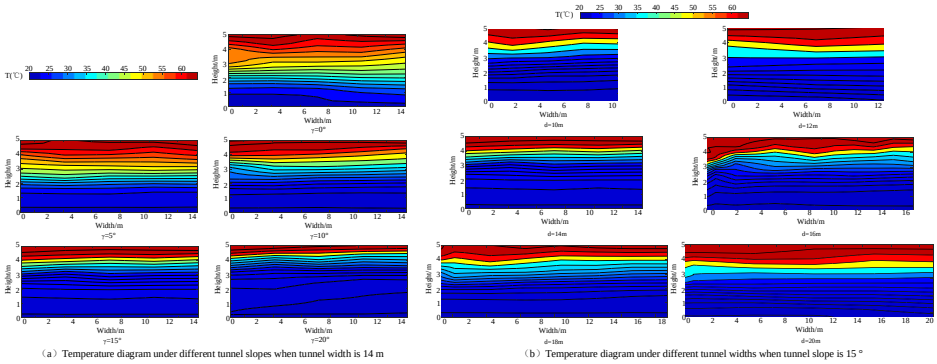

Fig. 7 Cross-sectional temperature distribution at a distance of 1 m from tunnel lower port

Fig. 8 shows the smoke countercurrent diagram in the upwind direction when tunnel width is 10 m, 12 m, 14 m, 16 m, 18 m and 20 m respectively when tunnel slope is 15 ° under natural ventilation condition in stable fire combustion stage. According to Fig. 8, upwind countercurrent length of fire smoke becomes longer with tunnel width's increase. As shown in Fig. 6 and Fig. 7 and Wang et al. [15], chimney effect's intensity decreases with tunnel width's increase, which has a certain impact on tunnel entrance's airflow velocity. Tunnel entrance's airflow velocity increases with tunnel width's narrowing while changes little when tunnel width is greater than 14m. Therefore, the upwind smoke countercurrent length increases with tunnel width's increase, but with tunnel width's increase, the effect of width on smoke countercurrent length decreases gradually.

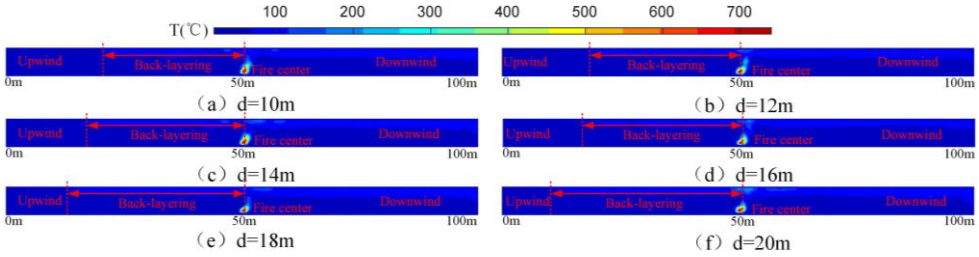

Fig. 8 Fire smoke countercurrent diagram of tunnels with different widths when tunnel slope is 15°

Fig. 9 shows the smoke countercurrent diagram in the upwind direction when tunnel slope is 0 °, 5 °, 10 °, 15 °and 20 ° respectively when tunnel width is 14 m under natural ventilation condition in stable fire combustion stage. It can be concluded from Fig. 9 that when tunnel is horizontal, fire smoke is uniformly distributed along the tunnel, and smoke countercurrent length is basically the same in fire source's upwind and downwind direction. As is visible from that analysis of Fig. 6 and Fig. 7 above, with tunnel inclination angle's increase, due to chimney effect's enhancement, tunnel entrance's air velocity increases, so that more fire smoke is blown downwind, and the upwind smoke countercurrent length decreases gradually.

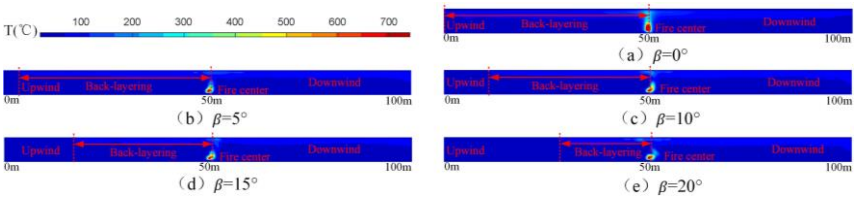

Fig. 9 Fire smoke countercurrent diagram of tunnels with different slopes when tunnel width is 14m

When a fire occurs in a mechanically ventilated tunnel with a certain slope, the main driving force for the flow of fire smoke is mechanical ventilation. Fig. 10 shows smoke countercurrent length in fire source's upwind direction when tunnel has different width and slope and longitudinal ventilation speed V = 1 m/s. It is visible from Fig. 10 that while there is mechanical ventilation, compared with natural ventilation, fire smoke countercurrent length decreases. Smoke countercurrent length decreases with tunnel slope's increase and increases with tunnel width's increase.

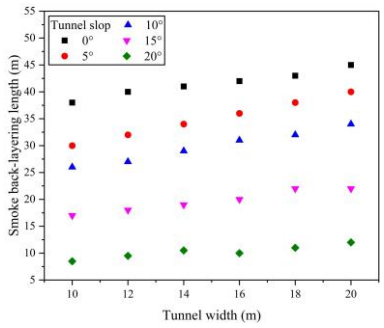

Fig. 10 Fire smoke countercurrent length diagram of tunnels with different widths and slopes

3.2. Theoretical Analysis of tunnel smoke countercurrent length

Thomas [39] first put forward the formula of smoke countercurrent length in tunnel fire in 1958:

$$L^* = \frac{L}{H} = \frac{gHQ}{\rho_a c_p T_a V^3 A} \tag{4}$$

In the formula, L^* is dimensionless smoke countercurrent length about tunnel height (m), L is tunnel smoke countercurrent length (m), A is tunnel cross-sectional area (m^2), and V is tunnel ventilation velocity (m/s).

Based on the above research, Vantelon et al. [40] analyzed smoke countercurrent length through heaps of reduced-size tunnel fire experiments and indicated it is associated with Richardson number, and modified the formula as follows:

$$L^* = \frac{L}{H} = \left(\frac{gHQ}{\rho_a c_p T_a V^3 A}\right)^{0.3} = Ri^{0.3} \tag{5}$$

In the equation: Ri represents Richardson number.

Subsequently, Li et al. [23] propounded the following formula to foretell tunnel fire smoke's counter-current length based on fire experiment and theoretical analysis:

$$L^* = \begin{cases} 18.5ln\left(0.81Q_c^{*\frac{1}{3}}/V_c^*\right) & Q_c^* \le 0.15 \\ 18.5ln(0.43/V_c^*) & Q_c^* > 0.15 \end{cases} \tag{6}$$

In the equation:

$$Q_c^* = \frac{Q}{\rho_a c_p T_a \sqrt{g} H^{\frac{5}{2}}} \tag{7}$$

$$V_c^* = \frac{V}{\sqrt{gH}} \tag{8}$$

Later, Weng et al. [10] put forward the formula of smoke countercurrent length in tunnel fire through scale-down experiment and numerical simulation analysis.

$$L^* = 7.13ln(0.81Q_c^*/V_c^{*3}) - 4.36 \tag{9}$$

In the equation:

$$Q_c^* = \frac{Q}{\rho_a c_p T_a \sqrt{g} \bar{H}^{\frac{5}{2}}} \tag{10}$$

$$V_c^* = \frac{V}{\sqrt{g\bar{H}}} \tag{11}$$

$\bar{H}$ is the height of tunnel water conservancy and its specific formula is:

$$\bar{H} = \frac{2Hd}{d+H} \tag{12}$$

Where, d is tunnel width (m).

Wan et al. [32] executed fire experiments on different tunnel slopes, and pointed out that the formula of tunnel fire smoke countercurrent length with respect to tunnel inclination angle is as follows:

$$L^* = \frac{L}{H} = 0.06\beta^{-1.57} \quad (13)$$

According to the above comprehensive analysis, smoke countercurrent length in tunnel fire is greatly influenced by the following factors. They are fire heat release rate Q , tunnel ventilation speed V , tunnel height H , tunnel width D , gravity acceleration G , ambient air density ρ_a, ambient air specific heat capacity c_p at constant pressure, ambient air temperature T_a and tunnel inclination angle β. Therefore, smoke countercurrent length and its influencing factors can be verbalized as:

$$f(L, H, d, Q, V, g, \rho_a, T_a, c_p, \beta) = 0 \quad (14)$$

In the dimensionless analysis, following the principle of π theorem, H, V, ρ_a and c_p are chosen as elementary dimensions for analysis, thus formula (14) can be transformed into the following formula:

$$f\left(\frac{L}{H}, \frac{d}{H}, \frac{Q}{H^2V^3\rho_a}, \frac{gH}{V^2}, \frac{c_pT_a}{V^2}, \beta\right) = 0 \quad (15)$$

The formula of smoke countercurrent length in tunnel can be verbalized as:

$$\frac{L}{H} = f\left(\frac{d}{H}, \frac{Q}{H^2V^3\rho_a}, \frac{gH}{V^2}, \frac{c_pT_a}{V^2}, \beta\right) \quad (16)$$

Then by merging the first four items, the formula (16) can be verbalized as:

$$\frac{L}{H} = f\left(\frac{Q}{\rho_a c_p T_a \sqrt{g} d H^{3/2}} \Big/ \left(\frac{V}{\sqrt{gH}}\right)^3, \beta\right) \quad (17)$$

The countercurrent length of dimensionless fire smoke is defined as:

$$L^* = \frac{L}{H} \quad (18)$$

The dimensionless longitudinal velocity V^* and dimensionless heat release rate Q^* of the tunnel width are:

$$Q^* = \frac{Q}{\rho_a c_p T_a \sqrt{g} d H^{3/2}} \quad (19)$$

$$V^* = \frac{V}{\sqrt{gH}} \quad (20)$$

Fig. 11 shows the relation among dimensionless fire smoke countercurrent length L^*, heat release rate Q^* and longitudinal velocity V^* when tunnel is arranged horizontally and longitudinal ventilation speed is 1m/s. The prediction formula of dimensionless smoke countercurrent length can be obtained from the diagram, the square difference R^2 is 0.99, and the overall fitting degree is high.

$$L^* = \frac{L}{H} = 3.64ln\left(\frac{Q^*}{V^{*3}}\right) - 2.51 \quad (21)$$

In order to compare and verify the prediction formula obtained in this paper with previous studies, the other curve in Fig. 11 corresponds to the full-scale tunnel fire experiment done by Liu [23], in which the tunnel width is 22 m and tunnel height is 5.1 m, from which the dimensionless smoke countercurrent length prediction formula is obtained. The results obtained in this paper are smaller than that obtained by Liu. Numerical models studied in this paper are large cross-section inclined tunnels and tunnel chimney effect increases with tunnel slope's change may be the mainspring.

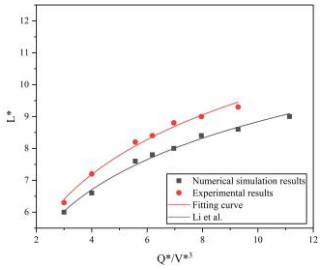

Fig. 11 Comparison diagram of dimensionless smoke countercurrent length L^* and Q^*/V^{*3} in horizontal tunnel when V=1m/s

Fig. 12 demonstrates the relation among dimensionless fire smoke countercurrent length L^*, heat release rate Q^* and longitudinal velocity V^* of the tunnel width for tunnels with a longitudinal ventilation velocity of 1 m/s and different inclined angles. As is visible from Fig. 12, when heat release rate is constant and longitudinal ventilation velocity is 1 m/s, countercurrent length gradually decreases with tunnel slope's increase. Due to gradual enhancement of air buoyancy caused by chimney effect, smoke buoyancy flow's direction is consistent with that of longitudinal ventilation, which can promote longitudinal ventilation and resist static pressure caused by fire. Therefore, the fire smoke countercurrent length in fire source's upwind direction decreases gradually.

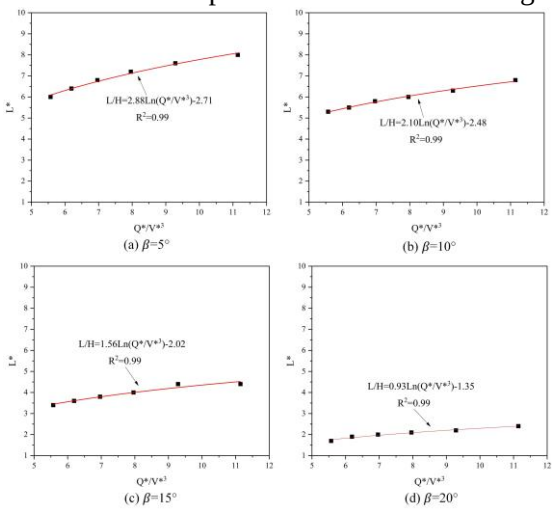

Fig. 12 Comparison diagram of dimensionless smoke countercurrent length L^* and Q^*/V^{*3} in different tunnel slopes when V=1m/s

3.3. Theoretical Analysis of tunnel critical velocity

Through previous studies and the above studies, with tunnel longitudinal ventilation velocity's increase, upwind diffusion's resistance of fire smoke increases. Then, when heat release rate is constant, smoke countercurrent length decreases gradually. Moreover, while longitudinal ventilation velocity rises to a definite value and fire smoke countercurrent length is 0 m, it is the critical velocity of longitudinal ventilation, then the formula (17) can be transformed into:

$$\frac{V^*}{Q^{*\frac{1}{3}}} = f(\beta) \qquad (22)$$

From the above analysis, it is visible that when fire smoke countercurrent length is 0 m, the formula of critical ventilation velocity for horizontal tunnel fire smoke not spreading upward can be obtained from the formula of smoke countercurrent length in Fig. 9, which can be expressed as:

$$V^* = 0.79Q^{*\frac{1}{3}} \qquad (23)$$

The critical velocity prediction formula obtained in this paper is compared with critical velocity prediction simulation model studied by Li et al. [23] and Weng et al. [10], as displayed in Fig. 13. Critical velocity is relatively lower compared with Li et al. and Weng et al. The main reason is that the tunnels studied in this paper are large in slope and width, and they are large-section tunnels. Therefore, the critical air volume needed to control the concentration of fire smoke to the downwind is reduced.

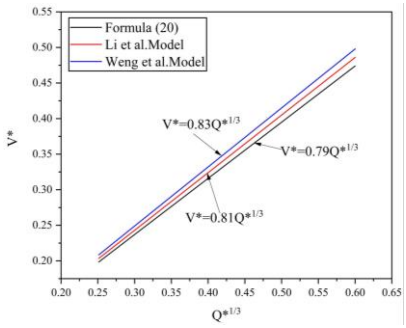

Fig. 13 Comparison between the formula for predicting critical ventilation speed of horizontal tunnel in this paper and previous research results when V=1m/s

From the above analysis, and according to dimensionless fire smoke countercurrent length formula in Fig. 12 when tunnel is inclined at different slopes, the fire smoke countercurrent length in different slopes is taken as 0 m. Then the corresponding critical velocity formula for controlling the fire smoke not to flow upward is obtained, as shown in Fig. 14. It is visible from Fig. 14 that when heat release rate is fixed, longitudinal mechanical ventilation is adopted and velocity is 1 m/s, with tunnel slope's increase, the minimum ventilation speed required to control upwind direction of fire smoke to produce countercurrent phenomenon, that is, the critical velocity, gradually decreases. This is due to the fact that with tunnel slope's increase, chimney effect caused by height difference increases and air buoyancy increases, fire smoke is hindered by air buoyancy caused by height difference when it flows upwind.

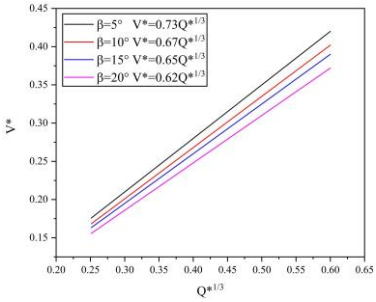

Fig. 14 Dimensionless critical velocity diagram of tunnel with different slopes under V=1m/s

From the above analysis, it is visible that critical velocity at which fire smoke countercurrent length is 0 m is different when tunnel slope is different, which is finally reflected in the difference of $f(\beta)$.

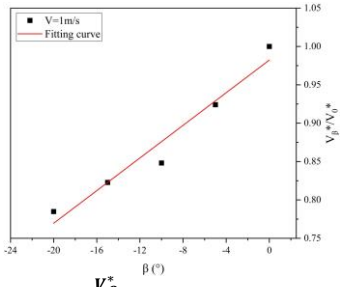

Fig. 15 Relationship between tunnel slope and $\frac{V_\beta^*}{V_0^*}$

Because this paper studies critical velocity in tunnel fire's upwind direction, that is, in the downhill direction. Therefore, if the slope is -5 °, -10 °, -15 °and -20 °respectively, the dimensionless relationship diagram of inclined tunnel's critical velocity V_β^*, horizontal tunnel's critical velocity V_0^*

and tunnel slope is displayed in Fig. 15. The relationship between the two can be obtained from the Fig. 13, and the fitting degree R^2 is 0.98.

$$\frac{V_\beta^*}{V_0^*} = 1 + 0.011\beta \quad (24)$$

In order to verify the critical velocity prediction formula procured in this paper, it is compared with the predicted critical velocity model procured by Chow et al. [15] and Atkinson et al. [41], as displayed in Fig. 16. As is visible from Fig. 16, the results of this paper are in good agreement with those of previous studies. Due to the different settings of tunnel longitudinal ventilation speed, tunnel slope and tunnel width, the results of this paper are slightly different from previous models, but the difference is small. The accuracy and reliability of the critical velocity prediction model of formula (24) are verified.

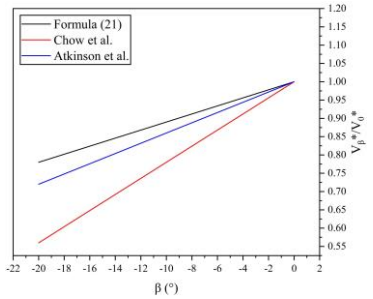

Fig. 16 Comparison between the formula (24) and previous studies

4. Conclusion

Based on the dimensionless analysis method and FDS numerical simulation method, this paper studies the effect of tunnel slope and width on the upwind smoke countercurrent length and critical velocity of tunnel fire. The specific conclusions are as follows.

(1) Under the conditions of natural ventilation and longitudinal ventilation, due to the chimney effect in the inclined tunnel, the chimney effect increases with large cross-section tunnel slope's increase, tunnel entrance's air velocity increases, and smoke countercurrent length decreases gradually in fire source's upwind direction. With large cross-section tunnel width's increase, tunnel entrance's airflow velocity decreases, and the upwind smoke countercurrent length gradually increases. However, with the tunnel width increases to 14-20 m, tunnel entrance's air velocity changes little, so the upwind smoke countercurrent length changes little.

(2) According to the characteristics of smoke countercurrent length in large cross-section tunnel fire under the condition of longitudinal ventilation, based on dimensionless analysis, the dimensionless expression of heat release rate considering tunnel width and height is modified, the prediction formula for smoke countercurrent length about tunnel slope, width and height under longitudinal ventilation is derived.

(3) With the large cross-section tunnel slope's increase, the tunnel critical velocity decreases gradually. Based on this, the relation between dimensionless critical velocity prediction expression and width, slope and height under longitudinal ventilation is modified, by comparing with previous research results, the reliability and accuracy of the formula are verified.

The smoke countercurrent length and the critical velocity of longitudinal ventilation in tunnel fire play important roles in fire prevention design and personnel evacuation. The research results of

this paper provide a certain theoretical basis for fire, tunnel ventilation and personnel rescue of large cross-section tunnels with different widths and slopes.

Acknowledgment

The research is supported by the National Natural Science Foundation of China (No. 51674016, 52004090). The authors are grateful for the support.

References

[1] Yao, Y.Z., *et al.,* Experimental study on the effects of initial sealing time on fire behaviors in channel fires. *International Journal of Thermal Science,* 125 (2018) 273-282.

[2] Guo, Y.H., *et al.,* Effect of Tunnel Cross Section on Smoke Stratification under Longitudinal Velocities. *Refrigeration & Air Conditioning,* 33 (06) (2019) 597-604.

[3] CTIF., World fire statistics. *International association of fire and rescue service,* (2018).

[4] Huang, Y.B., *et al.,* Experimental investigation on maximum gas temperature beneath the ceil ing in a branched tunnel fire. *International Journal of Thermal Science,* 145 (2019) 105997.

[5] Zhao, W.D., *et al.,* Influences of inclined tunnel ceiling on plug-holing phenomenon and mec hanical smoke exhaust efficiency in tunnel fires[J]. *Fire Mater,* 46 (5) (2021) 818-829.

[6] Chen, C.K., *et al.,* Experimental investigation on the influence of ramp slope on fire behavior s in a bifurcated tunnel. *Tunnelling and Underground Space Technology,* 104 (2020) 103522.

[7] Fan, C.G., *et al.,* Experimental study of air entrainment mode with natural ventilation using s hafts in road tunnel fire. *International Journal of Heat and Mass Transfer,* 56 (2013) 750-757 .

[8] Fei, T., *et al.,* A study on the maximum temperature of ceiling jet induced by rectangular-sour ce fires in a tunnel using ceiling smoke extraction. *International Journal of Thermal Science,* 127 (2018) 329-334.

[9] Ingason, H., *et al.,* Model scale tunnel fire tests with longitudinal ventilation. *Fire Safety Jour nal,* 45 (6) (2010) 371-384.

[10] Weng, M.C., *et al.,* Study on the critical velocity in a sloping tunnel fire under longitudinal ve ntilation. *Applied Thermal Engineering,* 94 (2016) 422–434.

[11] Weng, M.C., *et al.,* Prediction of backlayering length and critical velocity in metro tunnel fire s. *Tunnelling and Underground Space Technology,* 47 (2015) 64-72.

[12] Zhao, S.Z., *et al.,* A numerical study on smoke movement in a metro tunnel with a non-axisy mmetric cross-section. *Tunnelling and Underground Space Technology,* 73(Mar.) (2018) 187-202.

[13] Ingason, H., *et al.,* Model scale tunnel fire tests with point extraction ventilation. *Journal of F ire Protection Engineering,* 21(1) (2011).

[14] Wu, Y., *et al.,* Control of smoke flow in tunnel fires using longitudinal ventilation systems – a study of the critical velocity. *Fire Safety Journal,* 35 (4) (2000) 363-390.

[15] Chow, W.K., *et al.,* Chow. C.L, Miao. L, Smoke movement in tilted tunnel fires with longitud inal ventilation. *Fire Safety Journal,* 75 (2015) 14-22.

[16] Ji, J., *et al.,* Influence of cross-sectional area and aspect ratio of shaft on natural ventilation in urban road tunnel. *International Journal of Heat and Mass Transfer,* 67 (2013) 420-431.

[17] Ji, J., *et al.,* Effects of vertical shaft geometry on natural ventilation in urban road tunnel fires . *Journal of Civil Engineering and Management,* 20(4) (2014) 466-476.

[18] Fan, C.G., *et al.,* Smoke movement characteristics under stack effect in a mine laneway fire. *Applied Thermal Engineering,* 110 (2017) 70-79.

[19] Shafee, S., Yozgatligil. A, An analysis of tunnel fire characteristics under the effects of vehicu lar blockage and tunnel inclination. *Tunnelling and Underground Space Technology,* 79(SEP.) (2018) 274-285.

[20] Zhang, X.L., *et al.,* Numerical simulation on the maximum temperature and smoke back-laye ring length in a tilted tunnel under natural ventilation. *Tunnelling and Underground Space Te chnology,* 107 (2021) 103661.
[21] Thomas, P.H., The Movement of Smoke in Horizontal Passages against Air Flow. *Fire Resear ch Technical Paper,* 7 (1) (1968) 1-8.
[22] Oka, Y., *et al.,* Control of smoke flow in tunnel fires. *Fire Safety Journal,* 25 (4) (1995) 305-322.
[23] Li, Y.Z., *et al.,* Study of critical velocity and backlayering length in longitudinally ventilated t unnel fires. *Fire Safety Journal,* 45(6-8) (2010) 361-370.
[24] Hyun Ko, Q., *et al.,*An Experimental Study of the Effect of the Slope on the Critical Velocity in Longitudinal Tunnel Fires. (2005).
[25] Weng, M.C., *et al.,* Prediction of backlayering length and critical velocity in metro tunnel fire s. *Tunnelling and Underground Space Technology,* 47 (2015) 64-72.
[26] Yi, L., *et al.,* experimental study on critical velocity in sloping tunnel with longitudinal ventil ation under fire. *Tunnelling and Underground Space Technology,* 43 (1) (2014) 198-203.
[27] Li, Y.Z., *et al.,* Effect of cross section on critical velocity in longitudinally ventilated tunnel fi res. *Fire Safety Journal,* 91 (jul.) (2017) 303-311.
[28] Li, Y.Z., *et al.,* Discussions on critical velocity and critical Froude number for smoke control in tunnels with longitudinal ventilation. *Fire Safety Journal,* 99 (2018) 22-26.
[29] Li, J., *et al.,* A study on the effects of the slope on the critical velocity for longitudinal ventila tion in tilted tunnels. *Tunnelling and Underground Space Technology,* 89 (JUL.) (2019) 262-2 67.
[30] Jiang, L., *et al.,* Control of light gas releases in ventilated tunnels. *Journal of Fluid Mechanic s,* 872 (2019) 515-531.
[31] Chow, W.K., *et al.,* Chow. Nadia C.L, A study on tilted tunnel fire under natural ventilation. *Fire Safety Journal,* 81 (2016) 44-57.
[32] Wan, H.X., *et al.,* A numerical study on smoke back-layering length and inlet air velocity of f ires in an inclined tunnel under natural ventilation with a vertical shaft. *International Journal of Thermal Science,* 138 (2019) 293-303.
[33] Yang, X.L., *et al.,* Experimental investigation on the smoke back-layering length in a branche d tunnel fire considering different longitudinal ventilations and fire locations. *Case Studies in Thermal Engineering,* 28 (2021) 101497.
[34] Jiang, L., *et al.,* Effect of tunnel slope on the critical velocity of densimetric plumes and fire p lumes in ventilated tunnels. *Tunnelling and Underground Space Technology,* 123 (2022) 1043 94-.
[35] Ji, J., *et al.,* Experimental investigation on influence of different transverse fire locations on maximum smoke temperature under the tunnel ceiling, *International Journal of Heat and Ma ss Transfer,* 55 (17-18) (2012) 4817–4826.
[36] Mcgrattan, K., *et al.,* Fire Dynamics Simulator User's Guide. *National Institute of Standards and Technology,* Gaithersburg. Maryland. (2018).
[37] Long, X.F,, *et al.,* Numerical simulation of smoke pervasion in tunnel fire affected by ceiling flue, *Journal of University of Science and Technology of China,* 37 (4) (2009) 100–105.
[38] Ji, J., *et al.,* Large eddy simulation of stack effect on natural smoke exhausting effect in urban road tunnel fires, *International Journal of Heat and Mass Transfer,* 66 (2013) 531–542.

[39] Thomas, P.H., The movement of buoyant fluid against a stream and the venting of undergrou nd fires. *Fire Safety Science,* 351 (1958) -1--1.
[40] Jean-Vantelon., *et al.,* Investigation Of Fire-Induced Smoke Movement In Tunnels And Statio ns: An Application To The Paris Metro. *Fire Safety Science,* 3 (1991) 907-918.
[41] Liu, C., Study of ventilation control for fire-induced smoke in metro tunnel conjunction area. *Northeastern University,* (2019).
[42] Atkinson, G., *et al.,* Smoke control in sloping tunnels. *Fire Safety Journal,* 27 (1996) 335-34 1.

Submitted: 28.03.2023.
Revised: 10.07.2023.
Accepted: 17.08.2023.